Proceedings of the 6th International Charles Parsons Turbine Conference, Engineering Issues in Turbine Machinery, Power Plant and Renewables,
eds A. Strang, R. D. Conroy, W. M. Banks, M. Blackler, J. Leggett, G. M. McColvin, S. Simplson, M. Smith, F. Starr and R. W. Vanstone, Institute of Materials, London, 2003, 525--535

An affordable creep-resistant nickel-base alloy for power plant

F. Tancret[a] and H.K.D.H. Bhadeshia[b]

[a] Laboratoire Génie des Matériaux, Polytech' Nantes
[b] Department of Materials Science and Metallurgy, University of Cambridge, Pembroke Street, Cambridge CB2 3QZ, United Kingdom.

Introduction

Future fossil fuel power plant are being conceived to operate with steam temperatures as high as 750°C. This would increase the thermodynamic cycle efficiency, induce fuel savings and reduce polluting emissions. For these high temperatures, nickel-base superalloys are the prime candidates, but the price of commercially available alloys is too high for large scale power plant applications. In this aim, a new affordable nickel-base superalloy has been designed, with an expected creep rupture life of 100 000 h at 750°C under 100 MPa. The design requirements also included forgeability, weldability, corrosion resistance, and microstructural stability over long exposure at service temperature. This procedure resulted in considerable design time and costs savings compared to the usual "try-and-test" methods.[1]

The design procedure included the use of multiparameter non-linear regression techniques (Gaussian processes), coupled with superalloys databases, to model mechanical properties, and a thermodynamical simulation software (Thermo-Calc) to predict phase diagram, microstructural stability and solidification segregation. In the first part of this paper we will review quickly these design concepts and techniques.

This new alloy, with composition Ni-20Cr-3.5W-2.3Al-2.1Ti-5Fe-0.4Si-0.07C-0.005B (wt.%), has now been fabricated and thouroughly tested, in particular microstructure and high temperature mechanical properties —including creep tests up to more than 4 200 hours—, which will be presented in the second part of this work.

Finally, it is important to investigate the processablity of such an alloy, and to optimise fabrication processes. Consequently, some processing issues are dealt with in this paper, like modelling and characterisation of primary segragation during solidification —which is important for forging and welding processes—, and modelling and characterisation of precipitation ageing kinetics —which is important for heat treatment optimisation.

Modelling techniques and alloy design procedure

The influence of composition and processing parameters on the properties of materials is very complex and multivariate, so that designing an alloy "to-measure" is not feasible using

experience alone. Modern alloys contain many chemical elements added to achieve particular properties. The influence of individual alloying elements on mechanical properties can be measured and understood in isolated cases; and simple interactions can be formulated, but describing all the interactions as a whole is generally impossible. Recent papers[2,3] have demonstrated the possibility of using Gaussian processes to model the properties of materials as a function of their composition and/or processing parameters. They perform a non-linear multi-dimensional regression of an output (e.g. a mechanical property) as a function of many inputs (composition, thermomechanical treatments, temperature, etc.). Ideally, the database on which the model is based contains a large number of measurements, covering a wide range of alloy compositions and test conditions. It is not the aim of the present paper to explain how Gaussian processes work (this can be found in detail elsewhere[4]), but, basically, they perform a statistical analysis of the database and, to make a prediction, calculate the most probable value of the output given the whole database and the new set of inputs. Predictions are associated with an error bar, giving information on the level of confidence of the model.

For superalloys, quantitative predictive models were produced for yield stress, *Y*, ultimate tensile stress, *UTS*, tensile ductility, creep rupture stress, *CRS*, and γ/γ' lattice misfit, as a function of chemical composition, thermomechanical treatment and test conditions.[1,5]

The Gaussian processes models can predict mechanical properties, but they do not take into account any metallurgical knowledge about phase formation and stability. Thus, when used to predict the mechanical properties of a novel alloy, those models perform interpolations and/or extrapolations. Doing so, even if the methodology has often proved successful, it may happen that a non-desired phase forms in the novel alloy, which could not be predicted by the mechanical property models, and could be detrimental to the actual mechanical properties.[6]

For these reasons, we made use of a phase diagram and microsegregation computer simulation approach, as part of the design procedure of the new creep-resistant nickel-base superalloy. A thermodynamic simulation software, Thermo-Calc,[7] has been used in conjonction with a proprietary nickel-base superalloys database developped by Rolls-Royce plc. and Thermotec Ltd.. It can be used to predict the phases present as a function of temperature for a vast range of alloy compositions, and thus to check if undesirable phases —e.g. η and σ in superalloys— are to be expected or not.

The engineering requirements for the new alloy dictate a creep rupture life of 100 000 h at 750°C under a stress of 100 MPa, but there are other important design features which must be satisfied simultaneously. The *UTS* to *Y* ratio should be as high as possible, and in any case in excess of 1.3 at room temperature. The alloy must be easily forgeable and workable, i.e. it must be free of γ' for all temperatures within ~ 200 K of melting. Furthermore, the quantity of γ' must be less than ~ 25% in volume after heat treatment in order to ensure weldability[8] and ductility. Naturally, any such alloy must be able to cope with corrosive environments.

But an essential purpose of this work is price reduction with respect to existing alloys, which means that expensive elements (Co, Mo, Ta, Nb, Hf, Re…) must be avoided. Consequently, the proposed alloy will contain the following elements, for various reasons:

- A high Cr content, typically 20 wt.%, to achieve a good high temperature corrosion resistance.
- Al and Ti to form γ' precipitates, hence providing a precipitation strengthening effect.
- W, to induce a solid solution strengthening of both the γ matrix and γ' precipitates.
- C, to precipitate grain boundary carbides, which limit grain boundary sliding. Its content must, however, be small to avoid the formation of grain boundary carbide films, which are detrimental to creep resistance.[9] In this respect, 0.07 wt.% seemed an appropriate balance.
- B segregates at grain boundaries, and limits the grain boundary sliding mechanism.[9] Usual levels are around 0.005 wt.%.
- ~ 5 wt.% of Fe, to reduce cost. Pure Cr is very expensive, so ferrochrome or industrial scrap, which are both cheaper sources of Cr, will be used instead.
- A usual commercial alloy level of Si, i.e. 0.4 wt.%, which is a deoxidant.

Having fixed the contents of Cr, Fe, C, B and Si, predictions were made with various amounts of W, Al, and Ti. The latter were adjusted to find a compromise between a high creep rupture resistance, a low γ' volume fraction, a low γ/γ' lattice misfit, and no undesirable phase formation at the service temperature (750°C). The proposed composition is:

Ni - 20 Cr - 3.5 W - 2.3 Al - 2.1 Ti - 5 Fe - 0.4 Si - 0.07 C - 0.005 B, wt.%.

Heat treatment will consist of: 4 h at 1 175°C, 4 h at 935°C and 24 h at 760°C, with air cooling in all cases.

The predicted phase diagram of the designed alloy is presented in figure 1, on a three-scale plot of the molar amount of phases *versus* temperature. On the main scale, (top scale, 0 - 100%), the evolution of molar fractions of the principal phases, γ, γ' and liquid, has been plotted. The calculated liquidus, solidus, and γ' solvus are important for processing (forging and heat treatment). The expected γ' volume fraction at the service temperature of 750°C is 26 mol.%, which matches the criterion of a weldable superalloy. On the middle scale of figure 1, the calculated molar amounts of carbides are presented, which indicates the presence of $M_{23}C_6$ carbides at service temperature. These carbides precipitate at γ grain boundaries and improve creep resistance. On the bottom scale of figure 1, it can be seen that "TiB_2"-type borides are expected to form at high temperatures, and to dissolve at lower temperatures. However, this diagram results from equilibrium calculations, which do not take grain boundaries into account. Indeed, boron segregates at grain boundaries. Consequently, the formation of borides will have to be checked experimentally in the actual alloy. On the middle scale of figure 1, it can be seen that, under equilibrium conditions, a body-centered-cubic α-Cr phase is predicted to form below 690°C. This phase, even if similarly predicted in some chromium-rich commercial nickel-base superalloys, e.g. Nimonic 81, has not been reported to form. Additionally, the calculated formation temperature range of this α-Cr phase in the designed alloy is below 690°C, which is well below the expected service temperature. Finally, and this is one of the most important points, no other undesirable phases are expected to form in the vicinity of the service temperature. Phases like η, σ, or μ are detrimental for high-temperature mechanical properties, in particular for creep resistance.[10]

Microstructure and properties

Two 20 kg ingots of the designed alloy have been cast by Special Metals, and rolled to the shape of 30 mm diameter cylindrical bars. One of the bars was investigated in this study. The composition of the melt, from chemical analysis, is given in Table 1. It is rather close to nominal composition except for silicon, but this shouldn't affect mechanical properties too much. Concerning the strengthening elements, Al, Ti and W, they are a bit lower than target; carbon and chromium are slightly higher. Samples were cut out from the bar and heat-treated. In the following text, the samples subjected to the designed heat treatment are referred to as being "fully heat-treated".

A typical transmission electron microscope (TEM) micrograph of the fully heat-treated alloy is presented in figure 2. Spherical γ' precipitates of about 100 nm diameter can be seen within the γ grains. Grain boundaries are decorated with particle-like $M_{23}C_6$ carbides, as expected in the design procedure, which is desirable for a good creep resistance.

Compression yield stress of the fully heat-treated material was measured from the 0.2% plastic deformation offset on cylindrical specimens of 20 mm in length and 8 mm in diameter. Results are presented as a function of temperature in figure 3, and compared to the values predicted using the Gaussian processes model. A very good agreement between experimental and predicted values is obtained, on the whole temperature range. Measured values all lie within prediction error bars.

Creep tests were performed at 750°C on standard specimens with a gauge length of 25.4 mm and a diameter of 5.64 mm, for stresses of 320, 290, 260, 230 and 200 MPa. Results are plotted as a stress-lifetime graph in figure 4, along with the Gaussian processes predictions. Excellent agreement is obtained between predictions and experiments, which gives confidence in the statement that the alloy is likely to meet the intended engineering target of 100 000 h under 100 MPa at 750°C. Also, this validates the design procedure.

Processing issues

Solidification segregation

In order to process the material safely and efficiently —casting, forging, heat treatment, welding…—, it is important to investigate the alloy behaviour in this view. For instance, primary chemical segregation occurs during the solidification of alloys: dendrites grow with concentration gradients, and the final interdendritic medium composition is very different from nominal alloy composition. It has a low melting point, which can cause hot cracking during forging and/or welding.

A special module has been written within the Thermo-Calc software and used to simulate microsegregation during solidification, based on Scheil's approximation. The latter assumes a perfectly homogeneous liquid and a solid without diffusion. Starting from the liquid, temperature is decreased by small steps (1 K), and at each step a new liquid-solid equilibrium is calculated, the amount and composition of the liquid being kept as inputs fort the next step. The total amount of solid is the sum of solid quantities calculated at each step over the whole

process. This also allows the evolution of the liquid composition to be followed relative to the nominal alloy composition, to predict the composition gradients within dendrites and the primary segregation behaviour. Some of these have already been presented[1], but we will focus here on the dendrite concentration profiles. To model the latter, a simple dendrite shape must be assumed. In the present case, three shape models have been investigated: a plate, a cylinder and a sphere. At each computation step, the solidified volume, ΔV, and its composition are calculated. For the plate, cylinder and sphere models, respectively, the increase in dendrite thickness or radius, Δr, can be calculated with:

$$\Delta r_{plate} \quad \Delta V \qquad \Delta r_{cylinder} \quad \frac{\Delta V}{r} \qquad \Delta r_{sphere} \quad \frac{\Delta V}{r^2}$$

This has been related to the computed chemical composition of the solidifying material, and compared to actual concentration profiles in dendrite arms. Measurements have been performed by Energy Dispersive Spectroscopy (EDS) within a Scanning Electron Microscope (SEM). A typical dendrite micrograph is presented in figure 5, with the scan path along with the measurement has been made, from the core to the arm tip of the dendrite. A result is presented in figure 6 in the case of the titanium concentration profile. There is a rather good agreement between the spherical dendrite model and measurements, which validates the modelling approach.

Precipitation ageing kinetics

One major issue to optimise mechanical properties of Ni-base superalloys is to control the ageing heat treatment. Indeed, the desired γ' precipitates size, distribution and volume fraction must be attained, if possible with the simplest heat treatment possible. In the present design procedure, a three-step heat treatment, including two precipitation ageing treatments, was chosen. But it may be possible that equal mechanical properties can be obtained with a single-step ageing. To do so, γ' precipitation kinetics must be studied, understood and modelled. A preliminary investigation has been undertaken and the first results will be briefly presented. It combines several modelling approaches: a model of diffusion-controlled isothermal growth from a supersaturated solid solution, a thermodynamical simulation software, and a precipitation strengthening model.

First, the material is divided into elemetary volumes, each containing one growing precipitate. Before precipitation, the concentration in diffusive species (Al + Ti) is the nominal one, C_{nom}. It is assumed that during growth, at the precipitate/matrix interface, the concentration of diffusive species in the solid solution is given by thermodynamical equilibrium at the considered temperature, C_{eq}. The elementary volume is then divided into m slices of thickness dx. Initial conditions are thus: $C(1) = C_{eq}$ in this first slice, $C = C_{eq}$ in all other slices. A time step, dt, is chosen, during which the diffusive atom flux, $dN(i)$, moves from the $(i+1)^{th}$ slice to the i^{th} slice. It is computed following Fick's diffusion law, depending on the concentration gradient between the i^{th} slice and the $(i+1)^{th}$ slice:

$$dN(i) = -DS\frac{C(i) - C(i+1)}{dx}dt$$

where D is the effective diffusion coefficient and S the slice section. The number of diffusive atoms absorbed by the particle, dN_p, is calculated from the concentration gradient near the interface with:

$$dN_p = -DS\frac{C(1) - C(2)}{dx}dt$$

The concentration profile at time $t+dt$ in the solid solution, $C(i)_{t+dt}$, is then reevaluated by writing that the number of diffusive atoms in the i^{th} slice is equal to the previous number of atoms in the i^{th} slice ($C(i)_t.Sdx$), minus the number of atoms going to the $(i-1)^{th}$ slice, $dN(i-1)$, plus the number of atoms coming from the $(i+1)^{th}$ slice, $dN(i)$, so that:

$$C(i)_{t+dt} = C(i)_t - \frac{dN(i-1)}{Sdx} + \frac{dN(i)}{Sdx}$$

The total number of Al and Ti atom incorporating the particle, N_p, is then the sum of all dN_p calculated during the process. Each of these atoms pecipitates one $Ni_3(Al,Ti)$ lattice, which allows an estimate of the γ' volume fraction, V_f, as a function of ageing time.

Besides, a simple Freidel-type precipitation strengthening model is used to describe the increase in hardness, H, of the material as a function of V_f:

$$H = H_0 + A\sqrt{V_f}$$

Finally, this yields a model for the hardness of the material during the precipitation ageing process, with only two adjustable parameters: the effective diffusion coefficient, D, and the strengthening model proportionality constant, A.

The model was then compared to age-hardening measurements made at 750°C and 800°C. The material was first solutionised 4 h at 1175°C, water quenched, and its Vickers hardness, H_0, measured on a polished surface. Interrupted ageings were then made by heating specimens at 750°C or 800°C for various times, followed by water quenching. The Vickers hardness was then measured on polished surfaces. Measured hardnesses are presented in figure 7 as a function of ageing time, along with the developped model. The best fits are obtained with $D = 0.025\ nm^2/s$ at 750°C and $D = 0.20\ nm^2/s$ at 800°C, which also allows a rough estimate of the apparent activation energy for diffusion, Q, assuming that:

$$D = D_0 \exp\left(-\frac{Q}{RT}\right)$$

with D_0 a pre-exponential factor and R the gas constant. This yields Q = 380 kJ/mol, which is of the order of magnitude of values found in the literature for γ' growth[11], although measurements at several different temperatures would give better accuracy.

Conclusions

An affordable, forgeable, weldable, creep-resistant and corrosion-resistant nickel-base superalloy was designed using modern computing approaches (Gaussian processes modelling of mechanical properties, thermodynamical simulation). Both microstructure and mechanical properties are consistent with predictions; in particular, creep tests suggest that the alloy will match the engineering requirement of a lifetime of 100 000 h at 750°C under 100 MPa.

Preliminary modelling and experimental investigations were performed concerning processing issues. The primary solidification segregation behaviour was succesfully modelled using Scheil's approximation, and concentration profiles within dendrites could be predicted, which is important in view of forging and welding the alloy. Also, the precipitation hardening behaviour during ageing was described by an approach combining a diffusion-controlled

growth model, a thermodynamical simulation software and a simple strengthening model. This is useful in view of optimising the heat-treatment.

These studies need to be completed by further experimental investigations and models refinements —composition of the interdendritic medium, complex dendrite geometries, aeging at different temperatures, etc.

Further work will also include investigations about high temperature ductility and forgeability, recrystallisation, welding, etc.

References

1. F. Tancret, H.K.D.H. Bhadeshia *et al.*, *Materials Science and Technology*, 2003, in press.
2. C.A.L. Bailerjones, H.K.D.H. Bhadeshia and D.J.C. MacKay, *Materials Science and Technology*, 1999, **15(3)**, 287-294.
3. F. Tancret, H.K.D.H. Bhadeshia and D.J.C. MacKay, *ISIJ International*, 1999, **39(10)**, 1020-1026.
4. M.N. Gibbs, PhD Thesis, 1998, University of Cambridge, UK.
5. Materials Algorithms Project, http://www.msm.cam.ac.uk/map/
6. T. Cool: PhD thesis, 1996, University of Cambridge, UK.
7. Thermo-Calc, The Royal Institute of Technology, Stockholm, Sweden.
8. K.M. Chang and A.H. Nahm, *Superalloys 718 - Metallurgy and Applications*, ed. E.A. Loria, the Minerals, Metals & Materials Society, 1989, 631-646.
9. A.K. Jena and M.C. Chaturvedi: *Journal of Materials Science*, 1984, **19**, 3121-3139.
10. C.T. Sims: *Journal of Metals*, 1966, **18**, 1119-1130.
11. E. Balicki, A. Raman and R.A. Mirshams, *Metallurgical and Materials Transactions A*, 1997, **28**, 1993-2003.

	Cr	W	Al	Ti	Fe	Si	C	B
Nominal	20	3.5	2.3	2.1	5	0.4	0.07	0.005
Actual	20.28	3.308	2.22	1.978	5.025	0.053	0.102	0.0035

Table 1: Nominal and actual chemical composition of the new alloy (in weight %).

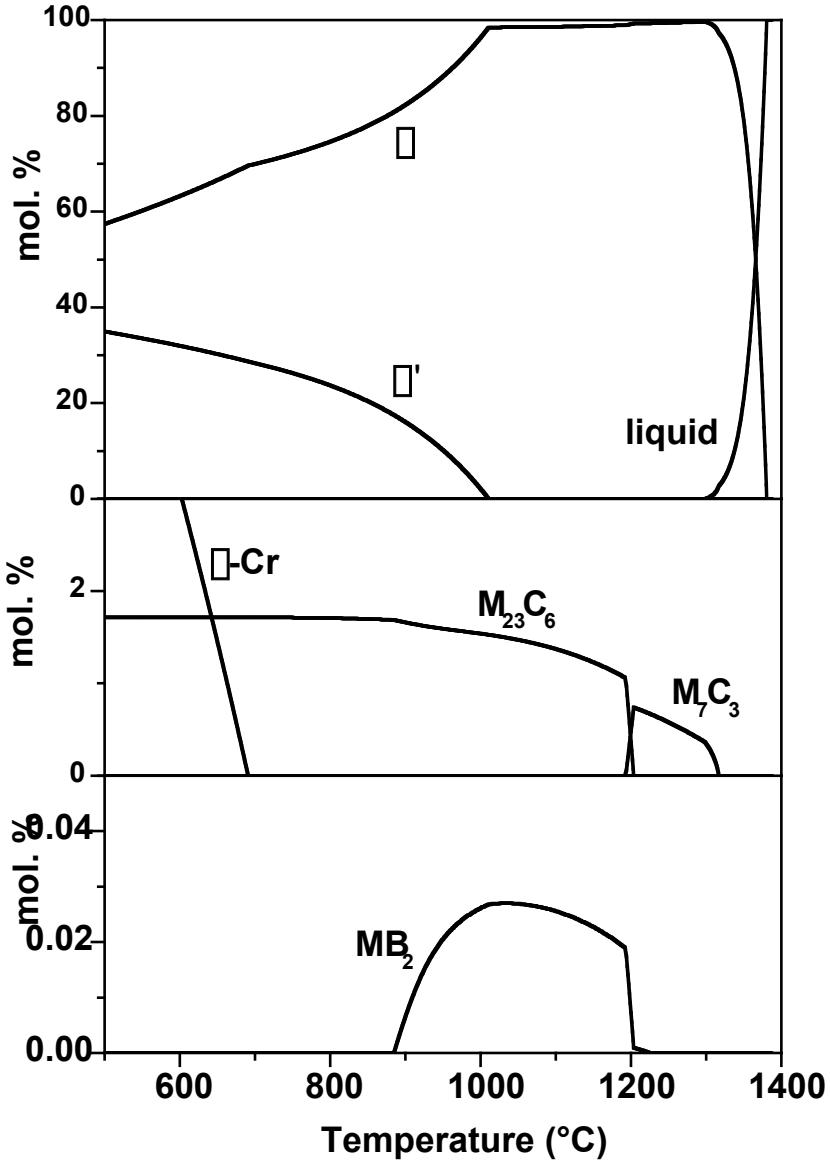

Figure 1: Calculated equilibrium phase diagram of the designed alloy.

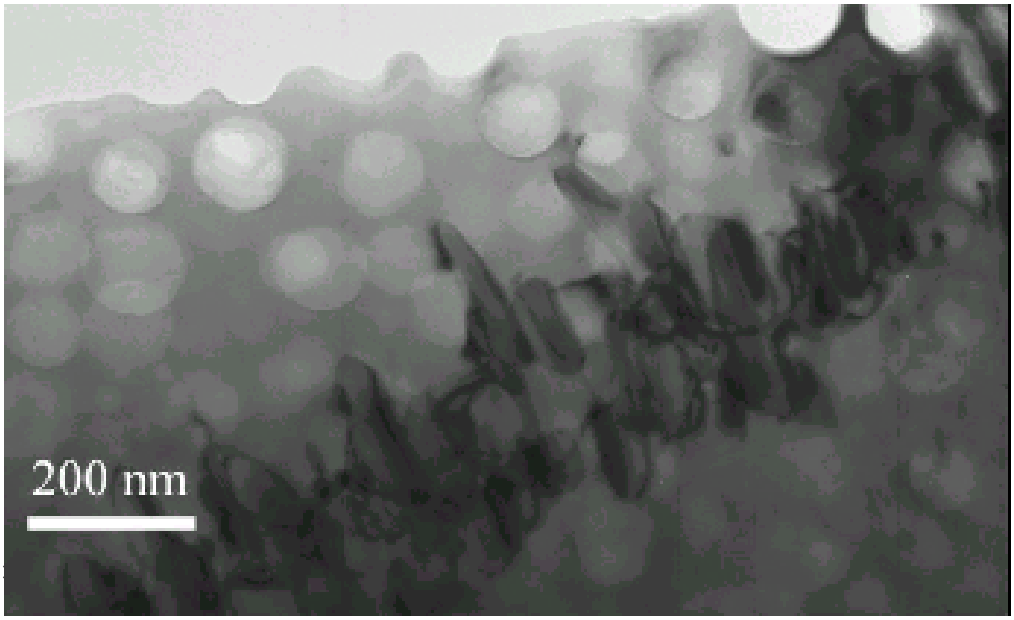

Figure 2

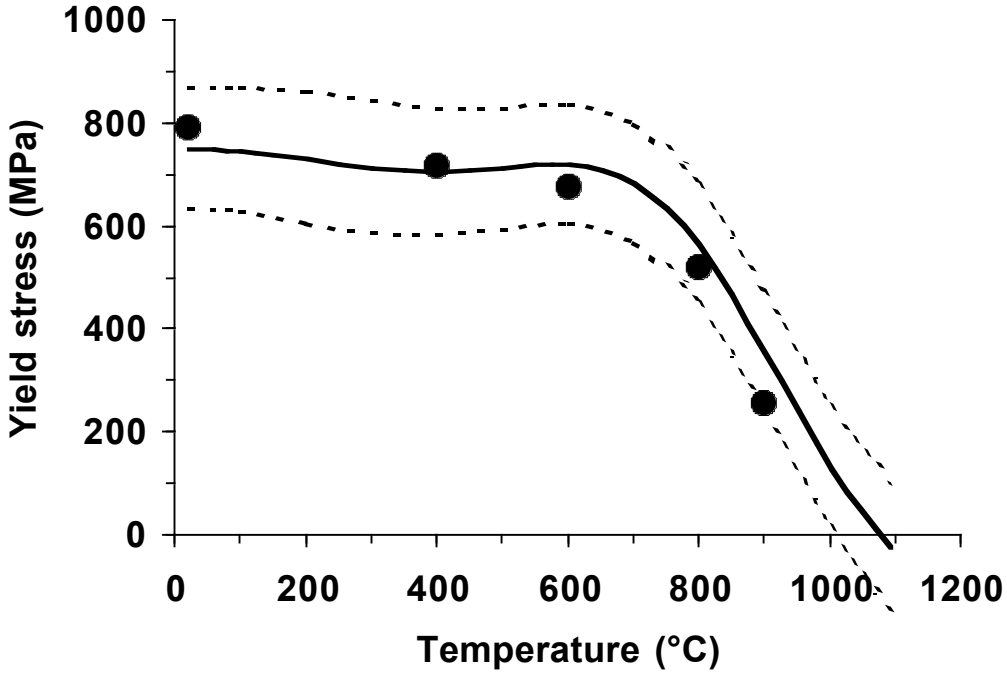

Figure 3: E
Gaussian pr

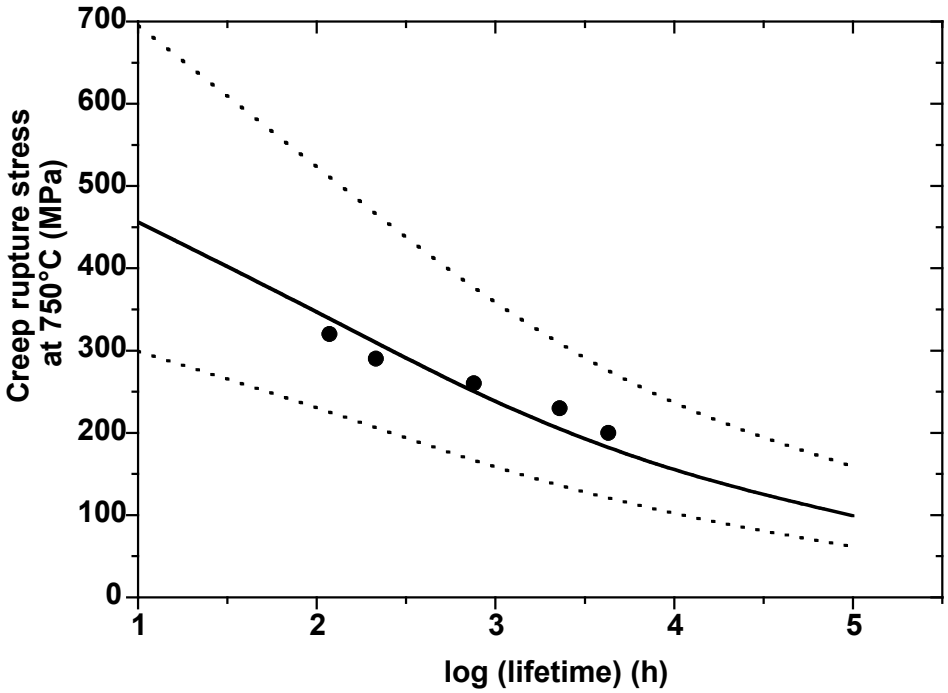

Figure 4: Creep rupture stress as a function of lifetime. Circles: measurements; solid line: mean Gaussian processes predictions; dotted lines: predicted error bounds.

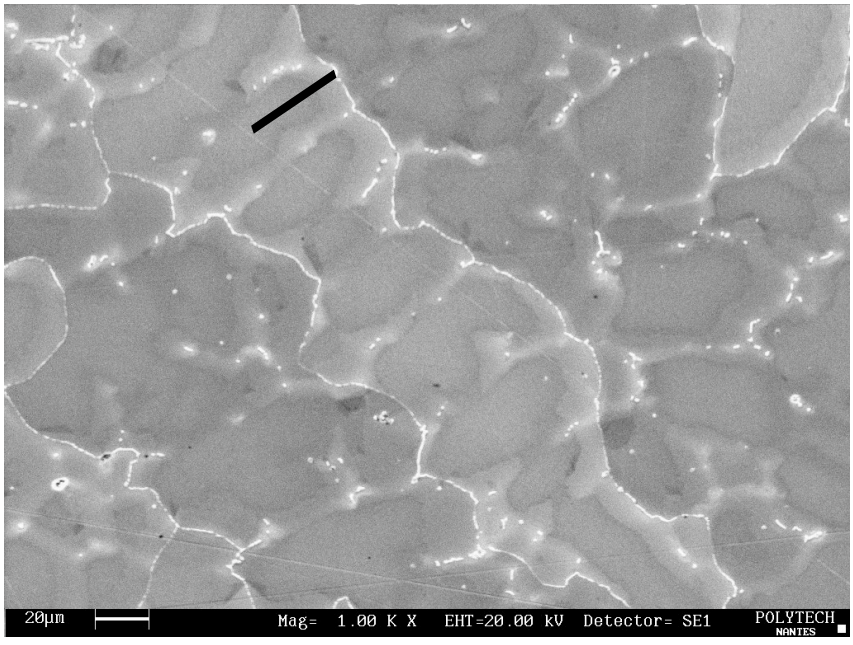

Figure 5: SEM micrograph of the as-solidified alloy. The black line is the EDS scan path.

Figure 6: Comparison between the predicted (right scale) and the EDS measured (left scale) titanium

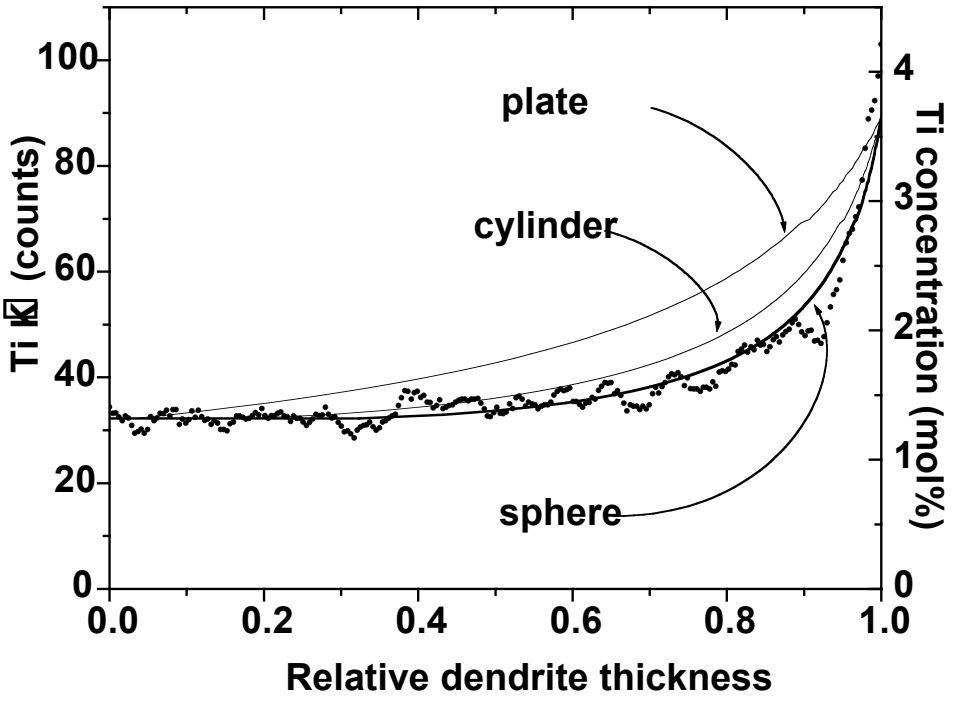

concentration profiles within dendrites, for different dendrite shape models.

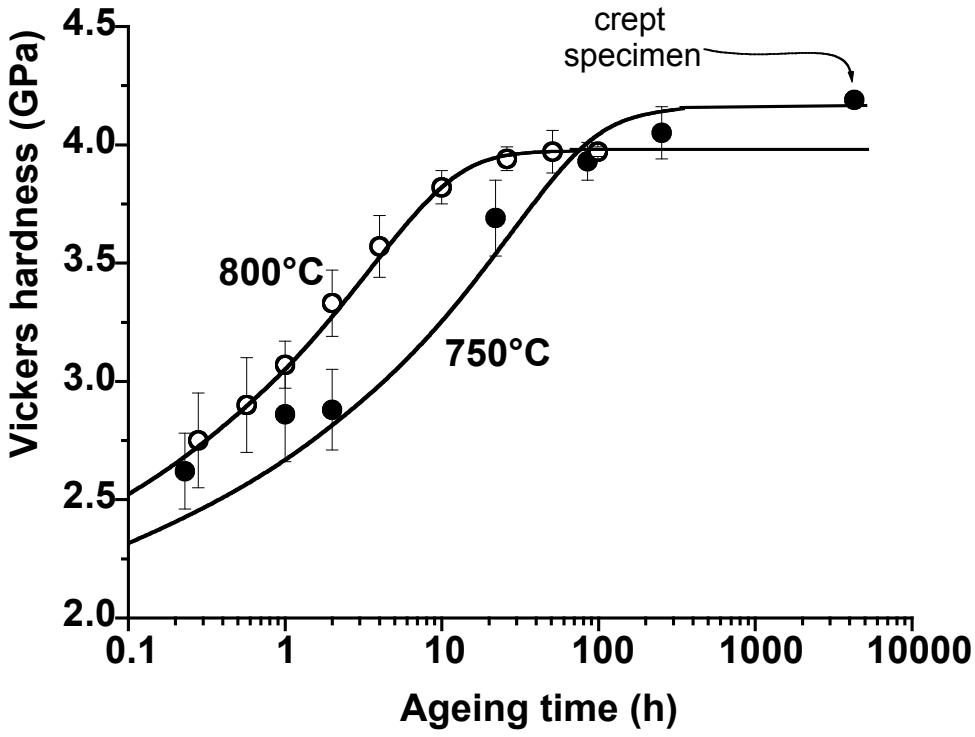

Figure 7: Evolution of Vickers hardness with ageing time. Symbols: experimental points; lines: model.